Energetics of quaternary III-V alloys described by incorporation and clustering of impurities

Koushik Biswas and Stephan Lany

National Renewable Energy Laboratory, Golden, Colorado 80401, USA

The energetics of alloy formation is generally modeled either by explicit sampling of the possible alloy configurations or by considering only noninteracting impurities in the dilute limit. We describe a model that bridges the two approaches by taking into account the thermodynamic probability to form small clusters by association of impurities, thereby extending the validity of the impurity model to higher concentrations. Since we express the alloy energetics in terms of pair and cluster binding energies there is no need for computationally intensive sampling over the full configuration space. The application to the $Ga_{1-x}In_xP_{1-y}N_y$ highlights the importance of short-range ordering due to "small atom/large atom" correlation in such quaternary III-V alloys.

I. INTRODUCTION

Quaternary III-V alloys of the type $A_{1-x}B_xC_{1-y}D_y$ provide a higher flexibility to engineer desirable optoelectronic properties than the more conventional ternary alloys of $A_{1-x}B_xC$ type.[1] These alloys are being extensively investigated for their applications in electronics as well as other developing fields such as frontiers of energy research. Recently, there have been attempts to utilize III-V nitride alloys for photoelectrochemical water splitting.[2–4] Incorporating N into III-V alloys has been shown to improve the optical and anticorrosive properties of these materials.[3,5] However, the large strain energy due to N incorporation limits its solubility and causes a lattice mismatch with the substrate that introduces additional defects and deteriorates the mechanical properties. Recent efforts are therefore concentrating on quaternary alloys such as $Ga_{1-x}In_xP_{1-y}N_y$ where the addition of lattice expanding In can counter the effects of mismatch caused by N incorporation.[1,4]

Compared to the traditional ternary alloys, such as GaInN or GaPN, there exist greater degrees of freedom for short-range ordering (SRO) in quaternary alloys with two cationic and two anionic constituents.[6–8] Such SRO affects the alloy energetics, hence the solubility and stability against phase separation, as well as the electronic and optical properties (band structure). While previous studies addressed the evolution of microstructure due to SRO,[6–9] here we examine also the effect of ordering on the alloy formation enthalpy and its solubility limit. To this end, we describe the alloy energetics from point of view of impurity incorporation in a host matrix. In the dilute concentration limit, the alloy energetics is governed by the formation energies ΔH_i associated with the substitution of the host site with the impurity atoms i (e.g., N_P i.e., N substituting a P atom) and alloy enthalpy ΔH_{alloy} is proportional to the alloy concentration $x_i = n_i / s_i$ (ratio of the density n_i of atoms i over the respective density s_i of available lattice sites),

$$\Delta H_{alloy} = \sum_i x_i \Delta H_i. \qquad (1)$$

The equilibrium concentrations x_i are given by the Boltzmann factor

$$x_i = \exp^{-\Delta H_i / kT}, \qquad (2)$$

where k is the Boltzmann constant. At higher concentrations, this picture of isolated noninteracting substitutional impurities breaks down and the alloy energy deviates from the linear behavior of Eq. (1). In this regime, the modeling of the alloy, including the effect of short-range order, is usually achieved by explicit sampling, e.g., through Monte Carlo simulations, of the different alloy representations in large supercells.[6] Even when the supercell energies are expressed by computationally efficient methods, such as valence-force field (VFF) (Refs. 10 and 11) or (dual-sublattice) cluster expansions,[12] the modeling of quaternary alloys by thermodynamic sampling at every point in the two-dimensional (x,y) composition space is often not practical.

Here, we present instead a model that aims to extend the range of validity of the dilute-impurity picture [Eqs. (1) and (2)], by taking into account impurity-impurity interactions and clustering. In contrast to related previous works,[13,14] our method is not restricted to a particular lattice type or nearest-neighbor bond distribution. Since we express the alloy energetics in terms of pair and cluster binding energies, no sampling over the full configuration space is necessary, and the enthalpies of those pairs and clusters can be evaluated with accurate but computationally more demanding methods such as density-functional theory. We show that this model can reliably predict the formation energy of quaternary ($Ga_{1-x}In_xP_{1-y}N_y$) and ternary ($GaP_{1-x}N_x$) alloys at compositions in excess of 10%, and use this model to demonstrate the dramatic influence of SRO on the quaternary alloy energy and the solubility limit.

II. MODEL

With increasing concentrations x_i, e.g., $x_1 = [In_{Ga}]$ and $x_2 = [N_P]$ in the quaternary $Ga_{1-x1}In_{x1}P_{1-x2}N_{x2}$ alloy, the probability increases to form pairs such as (In_{Ga}-N_P) or larger clusters such as ($2In_{Ga}$-N_P). One can determine a formation energy for these clusters and determine their relative concentrations x_c in a similar fashion like Eq. (2) by taking into account the number s_c of distinct cluster configurations per volume unit (see also Ref. 15), $x_c = n_c / s_c$. However, the simple addition of the total densities of all impurities and

clusters become inaccurate when low formation energies permit high impurity concentrations. In order to describe an alloy from the point of view of defect formation (e.g., impurity substitution) and subsequent pairing and clustering at higher concentration, one needs to take into account two effects that are omitted in the dilute limit. First, considering that the host atom h (e.g., Ga_{Ga}) can be viewed as a "defect" with zero formation energy, which leads to $x_h=1$, the sum of the concentration of impurity and host atoms exceeds the number of available lattice sites, i.e., the lattice sites are *overcounted*, and an appropriate normalization of Eq. (2) needs to be done. Second, the simple addition of isolated and paired/clustered occurrences of an impurity leads to *double counting* of impurities.

For illustration, we consider the example of a zinc-blende lattice in which the impurity atoms A and B substitute on the cation and anion site, respectively. Further, a close AB pair may form (the number of distinct configurations for the AB impurity cluster is $s_{AB}=4s_A=4s_B$), either due to a significant binding energy $-E_b>kT$, or simply statistically in a random distribution, e.g., in the limit of high temperature $-E_b \ll kT$. For the following model example, we consider the particular case that the formation enthalpies of impurities A and B are equal ($\Delta H_A=\Delta H_B$), and that the binding energy vanishes, $E_b=\Delta H_{AB}-\Delta H_A-\Delta H_B=0$. Of course, we are in general also interested in cases where $E_b \neq 0$, including the limit $E_b \ll 0$ in which the impurity concentrations are determined by the formation of the impurity pairs or clusters rather than by their isolated occurrence. In such a general case, the incorporation of A and B is correlated and the binding energy affects the equilibrium concentrations. A general model should be able to describe both limits, the uncorrelated ($E_b=0$) and the correlated ($E_b \ll 0$) incorporation.[16] Thus, in our illustrative model example with $E_b=0$, we determine the concentrations of A and B according to the conventional expression for the dilute limit, Eq. (2), and, since in general the formation of the AB pair also needs to be considered, we determine further the concentration of the AB pair from Eq. (2) using the formation energy $\Delta H_{AB}=\Delta H_A+\Delta H_B$. Finally, we simply add the isolated and paired occurrences of A and B, and show the concentrations $x_A=x_B$ in Fig. 1 ("addition") as a function of the formation energy $\Delta H_A=\Delta H_B$ (for $T=1000$ K). Since, in this example, we neglected the overcounting and double-counting effects mentioned above, x_A and x_B will be overestimated, as evident from the fact that the concentrations exceed the number of lattice sites when $\Delta H_A=\Delta H_B$ becomes smaller than about 0.1 eV (see Fig. 1).

On the other hand, in this particular model example, we can determine the "exact" concentrations $x_A=x_B$ (Fig. 1), simply by omitting the contribution from pair formation (since $E_b=0$) and correcting for the overcounting of lattice sites by means of a normalization, which accounts for the competition of all impurities i (here, just A or B) and the respective host atoms h on a given lattice site,

$$x_i^{ovc} = \frac{x_i}{\sum\limits_i x_i + x_h}, \qquad (3)$$

where the initial x_i (before normalization) are determined by Eq. (2) and $x_h=1$ as mentioned above.
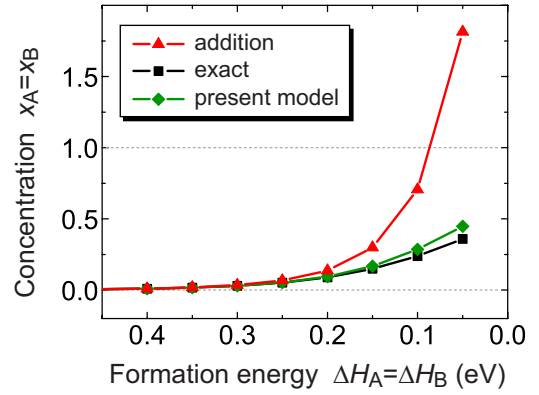

FIG. 1. (Color online) Example of a model alloy: total concentrations of impurities A or B as a function of their formation enthalpy. $\Delta H_A=\Delta H_B$ for the isolated A and B atoms, and $\Delta H_{AB}=\Delta H_A+\Delta H_B$ ($E_b=0$) for the close AB pairs. Triangles ("addition"): the concentrations are determined according to Eq. (2) and the isolated and paired occurrence of A and B are simply added. Squares ("exact"): the exact result for this particular model case. Diamonds ("present model"): the result obtained by accounting for overcounting and double-counting effects.

In order to describe the equilibrium concentrations in the general case, we need to take into account the thermodynamic balance between association and dissociation of clusters. For this purpose, we first determine the site concentrations $x_{i,c}$ for the impurities i that are part of a particular cluster c,

$$x_{i,c} = p_{i,c} \exp(-\Delta H_i/kT), \qquad (4)$$

where, $p_{i,c}$ is the statistical factor due to the *law of mass action* that includes also the effect of the reduced configurational entropy due to clustering. Note that $x_{i,c}$ can also be written in terms of $z_{i,c}$, the number of impurities i contained in one cluster c and the respective cluster concentration x_c,

$$x_{i,c} = z_{i,c} x_c s_c/s_i. \qquad (5)$$

We now illustrate for the example of formation of AB pairs how the factor $p_{i,c}$ is determined. For the lattice site occupied by the impurity A, we have $i=A$, $c=AB$, and $x_A=\exp(-\Delta H_A/kT)$, according to Eq. (2), before the normalization step of Eq. (3). Considering the law of mass action, $x_{AB}=x_A x_B \exp(-E_b/kT)$, and the relation $x_{A,AB}=x_{AB} \cdot s_{AB}/s_A$ [Eq. (5)] for the concentration of impurities A that are part of the AB pair, we obtain $p_{A,AB}=s_{AB}/s_A \cdot x_B \exp(-E_b/kT)$. The extension to larger clusters follows in a straightforward way from the general form of the law of mass action,

$$x_c = \exp(-\Delta E_b/kT) \prod_i x_i^{z_{i,c}}, \qquad (6)$$

in conjunction with Eqs. (4) and (5). At this point, Eq. (4) is nothing but the expression that gives the concentration of an impurity as part of a particular cluster when the cluster concentration is determined by the standard expression Eq. (2). However, this reformulation enables us to apply a *double-counting* correction after the addition of the isolated and

clustered occurrences of the impurity, $\tilde{x}_i = x_i + \Sigma_c x_{i,c}$ (e.g., $\tilde{x}_A = x_A + x_{A,AB}$)

$$x_i^{dcc} = \tilde{x}_i \left(1 - \frac{x_i}{\tilde{x}_i} \sum_c \frac{x_{i,c}}{\tilde{x}_i} \right). \qquad (7)$$

Here, the second term in the bracket accounts for the probability that the impurity i has been double counted as occurring both in the isolated form and as part of a cluster c (a similar expression can be formulated for the probability of double counting of the impurity i as being part of two or more clusters). In order to achieve self-consistency between the impurity and cluster concentrations, we first determine the isolated and clustered impurity concentrations by Eq. (4) [note that for isolated impurities, Eq. (4) reduces to Eq. (2)], then correct for double counting [Eq. (7)], and finally normalize according to Eq. (3). The resulting new impurity concentrations then enter the next cycle in Eq. (4) via the statistical factor $p_{i,c}$, and this procedure is iterated until the resulting concentrations of isolated impurities (on all sublattices) and the respective cluster concentrations are self-consistent in the sense that they observe the law of mass action, Eq. (6).

Applying the present model for the example shown in Fig. 1, we see that double-counting and overcounting effects are effectively removed and the range of validity is considerably extended toward higher alloy concentrations, compared to the conventional model (addition in Fig. 1), in which the isolated impurity concentrations are determined by Eq. (2) and the concentrations due to formation of pairs or clusters are simply added. Note that the conventional model is accurate only in two limits, i.e., when the number of impurities is small compared to the number of available lattice sites (no overcounting), and when the thermodynamic equilibrium is sufficiently far from the point where impurity association and dissociation are in competition with one another (no double counting). Also note that if electrically active impurities and defects (not considered in this work) are present, the equilibrium Fermi level can also be determined simultaneously during the self-consistency loop (see Ref. 17).

III. CALCULATION OF FORMATION ENERGIES

Our model describes the alloy formation by the incorporation of impurities into a host lattice, where the interaction (binding) between the impurities leads to the thermodynamic formation of impurity clusters. In order to compare this model with calculation of explicit alloy representations in large supercells, we use our recently developed generalized VFF method in which the energy functional parameters are obtained by fitting to first-principles (local-density approximation) calculated formation energies of a large set of ordered and random structures.[18] A brief description of the VFF energy functional and the fitted values of the quaternary alloy parameters (QVFF) are given in the Appendix. The formation energies of single substitutional impurities and their clusters, calculated in 1024 atom cells are given in Table I. Of course, once the validity of the present thermodynamic model is established, the impurity and cluster ener-

TABLE I. Calculated formation energies ΔH of isolated substitutional impurities in GaP (In_{Ga} and N_P) and that of impurity clusters. The binding energies E_b of the clusters are also given.

GaP	ΔH (eV)	E_b (eV)
In_{Ga}	0.18	
N_P	1.55	
In_{Ga}-In_{Ga}	0.38	+0.02
N_P-N_P	3.22	+0.12
In_{Ga}-N_P	1.10	−0.63
$2In_{Ga}$-N_P	0.75	−1.16
$3In_{Ga}$-N_P	0.49	−1.60
$4In_{Ga}$-N_P	0.34	−1.93
In_{Ga}-$2N_P$	2.14	−1.14

gies can also be determined from first-principles calculations in smaller cells,[19] which can be applied to a wider range of impurities, e.g., including electrically charged impurities.

IV. EFFECT OF SRO ON EQUILIBRIUM SOLUBILITY

The equilibrium solubility is calculated within the model described in Sec. II using the formation energies given in Table I (note that the formation energies implicitly include bounds of the chemical potentials for In and N due to the phase coexistence of GaN and InP). Figure 2 shows the equilibrium solubility limit of In and N in GaP, calculated with and without the effect of SRO due to clustering. In the latter case, there is no interaction between In_{Ga} and N_P ($E_b = 0$), and the resulting concentrations are equal to those when In or N are alloyed separately in GaP. Including the effect of SRO ($E_b \neq 0$, see Table I), we see that the N solubility is dramatically enhanced due to the possibility of In-N cluster formation when In is alloyed simultaneously. The N solubility of 4.2×10^{14} cm^{-3} without SRO increased to 1.9×10^{20} cm^{-3} in the presence of ordering with In at a temperature of 1000 K. In contrast, the In solubility remain relatively unaffected by additional N alloying (2.8×10^{21} with and 2.7×10^{21} cm^{-3} without SRO, respectively). This asym-
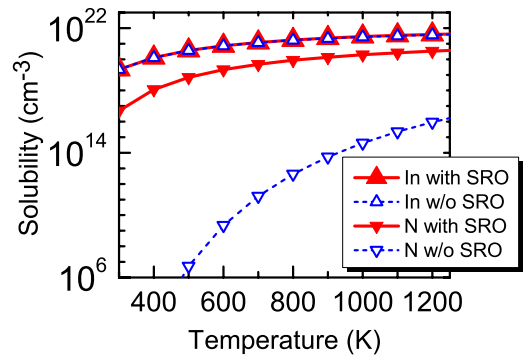

FIG. 2. (Color online) Equilibrium solubility of In and N in GaP matrix. Solid symbols correspond to alloy with clustering (with SRO) while open symbols denote random mixing (w/o SRO).
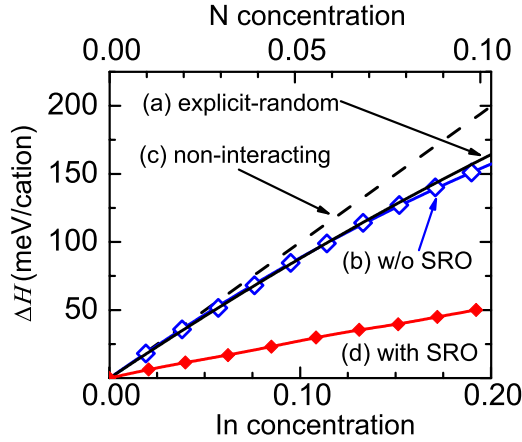
FIG. 3. (Color online) Formation enthalpy of $Ga_{1-x}In_xP_{1-y}N_y$ in the lattice matched ratio $x:y=2.12:1$. (a) Random alloy calculated with VFF in large supercells. (b) Present model for ΔH of the random alloy including statistical formation of clusters (w/o SRO). (c) ΔH due to noninteracting In_{Ga} and N_P impurities. (d) Present model for ΔH of the alloy with SRO at $T=1000$ K.

metry is a consequence of the different formation energies of the isolated In and N impurities: In_{Ga} has a relatively low formation energy (Table I), and, therefore, is abundant even without clustering with N_P (see Fig. 2). On the other hand, N_P has a high formation energy, leading to low concentrations. However, the large binding energies (Table I) and the relatively high In_{Ga} concentrations lead to a favorable statistical factor p in Eq. (4) for N_P occurring as part of a In-N cluster, which explains the dramatic enhancement of the N solubility due to simultaneous In alloying. Indeed, it is one of the advantages of the present method that this type of correlation is included and the In and N solubility limits are determined without any assumptions about the concentration of the respective other species.

V. FORMATION ENTHALPY (ΔH) OF THE QUATERNARY $Ga_{1-x}In_xP_{1-y}N_y$ ALLOY

Most of these alloys are grown by epitaxial techniques where it is possible to achieve lattice matching to a given substrate.[4,7,20] Here, we consider a $Ga_{1-x}In_xP_{1-y}N_y$ alloy with $x:y=2.12:1$, that conserves lattice matching to a GaP substrate and hence no energy contribution due to substrate strain. Figure 3 shows ΔH as a function of concentration of a random $Ga_{1-x}In_xP_{1-y}N_y$ ($x:y=2.12:1$) alloy as predicted by the generalized VFF model (see Appendix) utilizing a realistic random-alloy representation (averaged over ten random realizations at each concentration) in a large 4096-atom supercell [shown in Fig. 3(a)]. Figure 3(b) shows the present impurity-cluster model for the random alloy. Here, for the calculation of the relative concentrations of the isolated and clustered impurities, the binding energy is neglected ($E_b=0$, high-temperature limit), but the contribution to ΔH due the statistically formed clusters is taken into account. We see that this model reproduces the directly calculated random alloy [Fig. 3(a)] up to about 20% In (~10% N) substitution. Note that the ΔH corresponding to noninteracting impurities [i.e.,

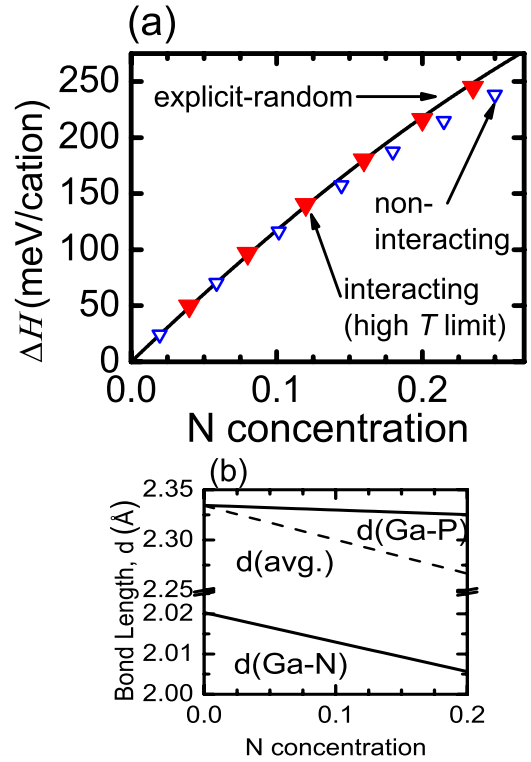FIG. 4. (Color online) (a) Formation enthalpy of $GaP_{1-x}N_x$ as a function of N concentration. Random alloy calculated with VFF in large supercell (explicit random, solid line). Present model for concentration-dependent ΔH of noninteracting N_P impurity (open triangles). Present model for concentration-dependent ΔH of interacting N_P impurity (solid triangles). (b) Variation in the average bond lengths as a function of N concentration.

if all impurities were isolated as in Eq. (1)] is strictly proportional to the alloy concentration and matches the initial slope of the directly calculated random alloy [Fig. 3(c)]. It is also important to point out that in this case of the lattice matched quaternary alloy (and therefore no associated strain contribution), the deviation of the formation enthalpy of the random alloy from a linear behavior as seen in Figs. 3(a) and 3(c) can be exclusively accounted for through the statistical probability of cluster formation and the related energy gain due to the impurity-cluster interactions.

Ternary alloys are often quite accurately described by the random-alloy model[18] where correlation effects, if any, can occur only between impurities (i.e., the foreign atoms that are alloyed into a host matrix) within the same sublattice. In contrast, in the case of dual-sublattice quaternary alloys like those considered here, correlation between the impurities on the cation and anion sublattice (i.e., pairing or clustering) can more directly affect the alloy energetics. Figure 3(d) shows the impurity-cluster model for $Ga_{1-x}In_xP_{1-y}N_y$, now including SRO for a temperature of $T=1000$ K. The binding energies (Table I) are now used to determine the thermodynamic equilibrium of cluster association/dissociation at this temperature. We see that the resulting alloy formation energy is dramatically reduced relative to the random alloy [see Figs. 3(b) and 3(d)]. This shows that the random-alloy approximation becomes entirely invalid, and the short-range ordering

due to "small atom/large atom" correlation, which causes considerable binding energies (Table I), strongly determines the alloy energetics in such quaternary III-V alloys.

VI. FORMATION ENTHALPY OF THE TERNARY $GaP_{1-x}N_x$ ALLOY

We now apply the present model to $GaP_{1-x}N_x$ as an example of a *ternary* alloy, where the assumption of random distribution is generally considered to be reasonably accurate,[18] in contrast to the present finding for the quaternary $Ga_{1-x}In_xP_{1-y}N_y$. Due to the large ($\sim$17%) lattice mismatch between the binary constituents of $GaP_{1-x}N_x$, we need to additionally take into account that the lattice constant of the host matrix changes during N substitution (unlike the case of the lattice matched quaternary alloy considered above). Thus, we calculate the formation energy of the isolated N_P impurity in a strained GaP supercell with a lattice constant such that the Ga-P distance equals the average Ga-P bond length in a random $GaP_{1-x}N_x$ alloy for a given concentration x [Fig. 4(b)]. Taking into account this concentration dependence of $\Delta H(N_P)$, but not the N_P-N_P "antibinding" energy (see Table I), already reproduces the enthalpy of the random $GaP_{1-x}N_x$ alloy quite well [Fig. 4(a)]. Including the statistical (high T limit) formation of N_P-N_P pairs and their concentration-dependent formation energy, almost exactly reproduces the random-alloy formation enthalpy [Fig. 4(a)], which again highlights the general applicability of our alloy model.

VII. CONCLUSION

We described a model for alloy energetics from point of view of impurity incorporation in a host matrix. The proposed model extends the validity of the dilute-impurity picture up to moderate alloy concentrations by taking into account the statistics and energetics of impurity-cluster association and dissociation, thereby avoiding the need for explicit sampling of alloy configurations. While the assumption of a random atomic distribution is often a good approximation in ternary alloys such as $GaP_{1-x}N_x$, the "preferential binding" of impurities to form clusters can lead to an atomic distribution very far from randomness. The binding between impurities to form pairs and clusters may drastically reduce the alloy enthalpy leading toward SRO. The application to

the $Ga_{1-x}In_xP_{1-y}N_y$ provides a quantitative picture about the effect of SRO on the formation enthalpies and solubility limits in quaternary III-V alloys.

APPENDIX

The quaternary valence-force-field model is based on an energy functional that includes bond-angle/bond-length interaction:[11]

$$U_{QVFF} = \sum_{i=1}^{N} \left\{ \sum_{j=1}^{4} \left[\frac{3}{16d_{ij}^2} \alpha_{ij}(\vec{r}_{ij} \cdot \vec{r}_{ij} - d_{ij}^2)^2 \right. \right.$$
$$\left. + \sum_{k=1,k\neq j}^{4} \frac{3}{16d_{ij}d_{ik}} \beta_{ijk}(\vec{r}_{ij} \cdot \vec{r}_{ik} - d_{ij}d_{ik}\cos(\theta_{ijk}^0))^2 \right] \right\}$$
$$+ \sum_{i=1}^{N} \sum_{j=1}^{4} \left[\sum_{k=1,k\neq j}^{4} \frac{3}{8d_{ij}\sqrt{d_{ij}d_{ik}}} \sigma_{ijk}(\vec{r}_{ij} \cdot \vec{r}_{ij} - d_{ij}^2) \right.$$
$$\left. \times (\vec{r}_{ij} \cdot \vec{r}_{ik} - d_{ij}d_{ik}\cos\theta_{ijk}^0) \right],$$

where α_{ij}, β_{ijk}, and σ_{ijk} are the bond-stretching, bond-bending, and bond-angle/bond-length interaction parameters, respectively. r_{ij} is the nearest-neighbor distance, d_{ij} is the ideal bond length, and θ_{ijk}^0 is the ideal unrelaxed tetrahedral bond angle (109.5°). For a given atom i, the indices j and k run over the four nearest-neighbor atoms in a zincblende lattice. For a given quaternary system, the α_{ij}, β_{ijk}, and σ_{ijk} are described through a set of 28 fitting parameters. These parameters were then fitted to first-principles calculated total energies of over 100 ordered and random-alloy structures. For a detailed description about the different parameters and the fitting methodology as well as the corresponding parameters for the (Ga,In) (P,N) ternary alloys (TVFF), see Ref. 18. The fitted values of the QVFF parameters are summarized in Table II.

TABLE II. Fitted QVFF parameters for the quaternary $Ga_{1-x}In_xP_{1-y}N_y$ alloy.

Alloy	d (Å)	α (N/m)	β (N/m)	σ (N/m)
			Fitted QVFF parameters	
GaInPN	d_{GaN}=1.931 d_{InN}=2.139 d_{GaP}=2.334 d_{InP}=2.524	α_{GaN}=46.5 α_{InN}=48.6 α_{GaP}=40.7 α_{InP}=33.4	$\bar{\beta}_{GaN}$=13.3; $\Delta\beta_{GaN}$=1.0 $\bar{\beta}_{InN}$=10.7; $\Delta\beta_{InN}$=1.1 $\bar{\beta}_{GaP}$=10.7; $\Delta\beta_{GaP}$=1.0 $\bar{\beta}_{InP}$=7.6; $\Delta\beta_{InP}$=1.0 β_{GaInN}=9.2, β_{GaInP}=1.3 β_{GaPN}=17.7, β_{InPN}=11.6	$\bar{\sigma}_{GaN}$=−17.1; $\Delta\sigma_{GaN}$=−1.1 $\bar{\sigma}_{InN}$=−9.9; $\Delta\sigma_{InN}$=−1.0 $\bar{\sigma}_{GaP}$=−1.8; $\Delta\sigma_{GaP}$=−1.0 $\bar{\sigma}_{InP}$=−4.1; $\Delta\sigma_{InP}$=−1.1 σ_{GaInN}=−23.8, σ_{GaInP}=−3.6 σ_{GaPN}=−21.4, σ_{InPN}=−15.4

[1] M. Kondow, K. Uomi, A. Niwa, T. Kitatani, S. Watahiki, and Y. Yazawa, Jpn. J. Appl. Phys., Part 1 **35**, 1273 (1996); C. W. Tu, J. Phys.: Condens. Matter **13**, 7169 (2001).

[2] T. Bak, J. Nowotny, M. Rekas, and C. C. Sorrell, Int. J. Hydrogen Energy **27**, 991 (2002).

[3] T. G. Deutsch, C. A. Koval, and J. A. Turner, J. Phys. Chem. B **110**, 25297 (2006).

[4] T. G. Deutsch, J. L. Head, and J. A. Turner, J. Electrochem. Soc. **155**, B903 (2008).

[5] M. Weyers, M. Sato, and H. Ando, Jpn. J. Appl. Phys., Part 2 **31**, L853 (1992).

[6] K. Kim and A. Zunger, Phys. Rev. Lett. **86**, 2609 (2001).

[7] V. Lordi, V. Gambin, S. Friedrich, T. Funk, T. Takizawa, K. Uno, and J. S. Harris, Phys. Rev. Lett. **90**, 145505 (2003).

[8] M. Albrecht, H. Abu-Farsakh, T. Remmele, L. Geelhaar, H. Riechert, and J. Neugebauer, Phys. Rev. Lett. **99**, 206103 (2007).

[9] O. Rubel, B. Kunert, S. D. Baranovskii, F. Grosse, K. Volz, and W. Stolz, Phys. Rev. B **74**, 195206 (2006).

[10] T. Takayama, M. Yuri, K. Itoh, and J. S. Harris, Jr., J. Appl. Phys. **90**, 2358 (2001).

[11] K. Kim, P. R. C. Kent, A. Zunger, and C. B. Geller, Phys. Rev. B **66**, 045208 (2002).

[12] P. D. Tepesch, G. D. Garbulsky, and G. Ceder, Phys. Rev. Lett. **74**, 2272 (1995).

[13] K. Onabe, J. Phys. Chem. Solids **43**, 1071 (1982).

[14] M. Ichimura and A. Sasaki, Phys. Rev. B **36**, 9694 (1987).

[15] J. E. Northrup and S. B. Zhang, Phys. Rev. B **47**, 6791(R) (1993).

[16] The case of repulsive interaction, $E_b > 0$, which effectively reduces the number of available lattice sites for the impurities, is expected to have a small effect on the equilibrium concentrations in the range of low to moderate impurity compositions, considered here.

[17] S. Lany, Y.-J. Zhao, C. Persson, and A. Zunger, Appl. Phys. Lett. **86**, 042109 (2005).

[18] K. Biswas, A. Franceschetti, and S. Lany, Phys. Rev. B **78**, 085212 (2008).

[19] S. Lany and A. Zunger, Phys. Rev. B **78**, 235104 (2008).

[20] H. P. Hsu, P. Y. Yu, Y. S. Huang, S. Sanorpim, K. K. Tiong, R. Katayama, and K. Onabe, J. Phys.: Condens. Matter **19**, 096009 (2007).